

# MASSIVE PARTICLE DECAY AND COLD DARK MATTER ABUNDANCE

---

C. PALLIS

SISSA / I.S.A.S.,  
Via Beirut 2-4,  
34013 Trieste, ITALY

Physics Division, School of Technology,  
Aristotle University of Thessaloniki,  
540 06 Thessaloniki, GREECE  
e-mail address: kpallis@auth.gr

**ABSTRACT:** The decoupling of a cold relic, during a decaying-particle-dominated cosmological evolution is analyzed, the relic density is calculated both numerically and semi-analytically and the results are compared with each other. Using plausible (from supersymmetric models point of view) values for the mass and the thermal averaged cross section times the velocity of the cold relic, we investigate scenarios of equilibrium or non equilibrium production. In both cases, acceptable results for the dark matter abundance can be obtained, by constraining the reheat temperature of the decaying particle, its mass and the averaged number of the produced cold relic.

**Keywords:** Cosmology, Dark Matter

**PACS codes:** 98.80.Cq, 95.35.+d

---

## CONTENTS

1. INTRODUCTION	1
2. DYNAMICS OF MASSIVE PARTICLE DECAY	3
2.1 RELEVANT BOLTZMANN EQUATIONS . . . . .	3
2.2 NUMERICAL INTEGRATION . . . . .	4
2.3 SEMI-ANALYTICAL APPROACH . . . . .	4
3. COLD DARK MATTER ABUNDANCE	5
3.1 REFORMULATION OF BOLTZMANN EQUATIONS . . . . .	5
3.2 NON-EQUILIBRIUM PRODUCTION . . . . .	6
3.3 EQUILIBRIUM PRODUCTION . . . . .	7
3.4 THE CURRENT ABUNDANCE . . . . .	8
4. APPLICATIONS	9
4.1 EQUILIBRIUM VERSUS NON-EQUILIBRIUM PRODUCTION . . . . .	10
4.2 NUMERICAL VERSUS SEMI-ANALYTICAL RESULTS . . . . .	11
4.3 ALLOWED REGIONS . . . . .	13
5. CONCLUSIONS-OPEN ISSUES	15

## 1. INTRODUCTION

The enigma of the Cold Dark Matter (CDM) constitution of the universe becomes more and more precisely defined, after the recently announced WMAP results [1, 2], which determine the CDM abundance,  $\Omega_{\text{CDM}} h^2$  with an unprecedented accuracy:

$$\Omega_{\text{CDM}} h^2 = 0.1126^{+0.0161}_{-0.0181} \quad (1.1)$$

at 95% confidence level. In light of this, the relic density of any CDM candidate  $\tilde{\chi}$ ,  $\tilde{\chi} h^2$  is to satisfy a very narrow range of values:

$$\text{a) } 0.09 \lesssim \tilde{\chi} h^2 \quad \text{and} \quad \text{b) } \tilde{\chi} h^2 \lesssim 0.13 \quad (1.2)$$

which tightly restricts the parameter space of the theories which support the existence of  $\tilde{\chi}$ . The most popular of these are the R-parity conserving supersymmetric (SUSY) theories which identify  $\tilde{\chi}$  to the stable lightest SUSY particle (LSP) [3]. According to the standard scenario,  $\tilde{\chi}$  decouples from the cosmic fluid during the radiation-dominated era, being non-relativistic and in chemical equilibrium with plasma. The latter condition is satisfied naturally by the lightest neutralino of the minimal SUSY standard model (MSSM), which turns out to have the required strength of interactions, being weakly interacting.

Although quite compelling, this scenario comes across with difficulties, especially when it is applied in the context of economical and predictive versions of MSSM. E.g., in most of

the parameter space of the Constrained MSSM (CMSSM) [4],  $\tilde{\chi}$  turns out to be bino and its  $\Omega_{\tilde{\chi}} h^2$  exceed the bound of Eq. (1.2b). Several suppression mechanisms of  $\Omega_{\tilde{\chi}} h^2$  have been proposed so far: Bino-sleptons [5] and particularly, for large  $\tan \beta$ , bino-stau [6], bino-stops [7] or bino-chargino [8] coannihilations and/or A-pole effect [9] can efficiently reduce  $\Omega_{\tilde{\chi}} h^2$ . Also several kinds of non-universality in the Higgs [10] or gaugino [11, 12] and/or fermionic sector [13] can help in the same direction, creating additional coannihilation effects. As is expected, a more or less tuning of the SUSY parameters is needed in these cases, without a simultaneous satisfaction of other phenomenological constraints to be always possible (see, e.g. Ref. [2]). On the other hand,  $\Omega_{\tilde{\chi}} h^2$  turns out to be lower than the bound of Eq. (1.2a) in other models, e.g., in the anomaly mediated SUSY breaking model (AMSBM) where  $\tilde{\chi}$  is mostly wino [14] or in models based on SU(5) gaugino non-universality [15], where  $\tilde{\chi}$  can be higgsino. Then we have to invoke another CDM candidate, in order for the range of Eq. (1.2) to be fulfilled.

However, this picture can dramatically change, if the initial assumption of the standard scenario is lifted. Indeed, since there is no direct information for the history of the Cosmos before the epoch of nucleosynthesis (i.e., temperatures  $T > 1 \text{ M eV}$ ) the decoupling of  $\tilde{\chi}$  can occur not in the radiation-dominated era. As was pointed out a lot years before [16] and recently [17, 18], the  $\tilde{\chi}$  decoupling can be related to the decay of a massive scalar particle. The modern Cosmology theories are abundant of such fields, e.g. in aton [19], dilatons or moduli [20, 21], q-balls [22] (see, also [23]). During their decay, these particles perform coherent oscillations "reheating" the universe [24]. This phenomenon is not instantaneous [25, 19]. In particular the maximum temperature during this period is much larger than the so called reheat temperature, which can be better considered as the largest temperature of the radiation-dominated era [17]. Consequently, the "freeze out" of  $\tilde{\chi}$  could be realized before the completion of the reheating. The cosmological evolution during this phase is strongly modified as regards the standard one [24], with crucial consequences to  $\Omega_{\tilde{\chi}} h^2$  calculation [17, 18, 21, 26]. Namely, two types of  $\tilde{\chi}$ -production emerge, in contrast with the standard scenario: The equilibrium (EP) and the non equilibrium production (non-EP). We find that in both cases, comfortable satisfaction of Eq. (1.2) can be achieved, by constraining the reheat temperature, the mass of the decaying particle and the averaged number of the produced  $\tilde{\chi}$ , without any tuning of the SUSY parameter space. In other words, non standard Cosmology can liberate the Phenomenology of SUSY models from a very disturbing constraint.

In this paper we extend the analysis in Ref. [17], including the possibility that the decaying particle can directly decay to  $\tilde{\chi}$ . The problem has already been faced in Refs [21, 26], but without the consequences of the non standard cosmological evolution before reheating to be stressed. Although our analysis is oriented to the LSP  $\tilde{\chi}$ , it can become applicable to any CDM candidate.

In secs 2 and 3, the problem is solved both numerically and semi-analytically and the results are compared with each other in sec. 4. There, we realize, also, a model independent application of our findings in the case of SUSY models inspired  $\tilde{\chi}$  masses and cross sections. Throughout the text and the formulas, brackets are used by applying disjunctive correspondence and natural units ( $\hbar = c = k_B = 1$ ) are assumed.

## 2. DYNAMICS OF MASSIVE PARTICLE DECAY

We consider a scalar particle with mass  $m$ , which decays with a rate  $\Gamma$  into radiation, producing an average number  $N_{\sim}$  of  $\sim$  particles with mass  $m_{\sim}$ . We, also, let open the possibility (contrary to Ref. [21]) that  $\sim$  are produced through thermal scatterings in the bath. The theoretical analysis of the problem is presented in sec. 2.1 and its numerical treatment in sec. 2.2. Useful approximated expressions are derived in sec. 2.3.

### 2.1 RELEVANT BOLTZMANN EQUATIONS

The energy density of radiation  $\rho_R$  and the number densities of  $\phi$ ,  $n$  and  $\sim$ ,  $n_{\sim}$  satisfy the following Boltzmann equations [19, 21] (we use the shorthand  $\dot{\rho} = (\dot{m} - N_{\sim} \dot{m}_{\sim}) = \dot{m}$ ):

$$\dot{n} + 3Hn + \Gamma n = 0; \quad (2.1)$$

$$\dot{\rho}_R + 4H\rho_R - m n - 2m_{\sim} h_{\sim} v_{\sim} n_{\sim}^2 - n_{\sim}^{\text{eq}2} = 0; \quad (2.2)$$

$$\dot{n}_{\sim} + 3Hn_{\sim} + h_{\sim} v_{\sim} n_{\sim}^2 - n_{\sim}^{\text{eq}2} - N_{\sim} n = 0; \quad (2.3)$$

where dot stands for derivative with respect to (wrt) the cosmic time  $t$ ,  $h_{\sim} v_{\sim}$  is the thermal-averaged cross section of  $\sim$  particles times velocity and  $H$  the Hubble expansion parameter which is given by ( $M_P = 1.22 \cdot 10^{19}$  GeV is the Planck scale):

$$H^2 = \frac{8}{3M_P^2} (\rho_{\phi} + \rho_R + \rho_{\sim}); \quad \text{with } \dot{\rho}_{\phi} = m \dot{n} \quad \text{and} \quad \rho_{\sim} = m_{\sim} n_{\sim}; \quad (2.4)$$

The equilibrium number density of  $\sim$  obey the Maxwell-Boltzmann statistics:

$$n_{\sim}^{\text{eq}} = \frac{g}{(2\pi)^{3/2}} \frac{T^{3/2}}{m_{\sim}^3} e^{-m_{\sim}/T} P_n(m_{\sim}/T); \quad (2.5)$$

where  $g = 2$  is the number of degrees of freedom of  $\sim$  and  $P_n(z) = 1 + (4n^2 - 1)z + \dots$  is the polynomial part of the modified Bessel function of the second kind of order  $n$ ,  $K_n$ .

The temperature,  $T$  and the entropy density,  $s$  can be found using the relations:

$$\text{a) } \rho_R = \frac{2}{30} g T^4 \quad \text{and} \quad \text{b) } s = \frac{2}{45} g_s T^3; \quad (2.6)$$

where  $g(T)$  [ $g_s(T)$ ] are the energy [entropy] effective number of degrees of freedom at temperature  $T$ . Their numerical values are evaluated by using the tables included in micrOMEGAS [27], originated from the DarkSUSY package [28].

Central rôle to our investigation plays the reheat temperature. Its precise value,  $T_{\text{rh}}$  can be found, by solving numerically the following [29]:

$$\rho_R(T_{\text{rh}}) = \rho_{\phi}(T_{\text{rh}}); \quad (2.7)$$

However, following Ref. [17], we prefer to handle reheat temperature as an input parameter,  $T_{\text{RH}}$ , defining it through an analytic formula, which, however approximate fairly (within 10%)  $T_{\text{rh}}$ . This can be succeeded in terms of  $\Gamma$ , using the conventional expression [25, 29]:

$$T_{\text{RH}} = \frac{4}{45} \frac{r}{M_P} \frac{3g(T_{\text{RH}}) T_{\text{RH}}^2}{M_P} \quad (2.8)$$

Note that Eq. (2.8) differs from the corresponding definition in Ref. [17] by a factor 2 in the  $\Gamma = 1$  limit (our choice is justified in sec. 4.1).

## 2.2 NUMERICAL INTEGRATION

The numerical integration of Eqs (2.1)-(2.3) is facilitated by absorbing the dilution terms. To this end, we convert the time derivatives to derivatives with the scale factor,  $R$  [19, 17]. We find it convenient to define the following dimensionless variables:

$$f = n R^3; \quad f_R = \dot{n} R^4 \quad \text{and} \quad f_{\sim}^{\text{eq1}} = n_{\sim}^{\text{eq1}} R^3 : \quad (2.9)$$

In terms of these variables, Eqs (2.1)-(2.3) become:

$$\frac{df}{dR} = -\frac{f}{H R}; \quad (2.10)$$

$$\frac{df_R}{dR} = -m \frac{f}{H} + 2m_{\sim} h_{\text{vi}} \frac{f_{\sim}^2 - f_{\sim}^{\text{eq2}}}{H R^3}; \quad (2.11)$$

$$\frac{df_{\sim}}{dR} = h_{\text{vi}} \frac{f_{\sim}^2 - f_{\sim}^{\text{eq2}}}{H R^4} + N_{\sim} \frac{f}{H R}; \quad (2.12)$$

where

$$H = \frac{r}{3} \frac{1}{M_{\text{P}}} R^{-3/2} (m f + f_R + m_{\sim} f_{\sim})^{1/2} : \quad (2.13)$$

Since at early times the energy density of the universe is completely dominated by this field,  $m_{\sim} n_{\sim}$ , the system of Eqs (2.10)-(2.12) is solved, imposing the following initial conditions:

$$f(R_I) = n_I R_I^3 \quad \text{and} \quad f_R(R_I) = f_{\sim}(R_I) = 0; \quad \text{with} \quad R_I = m^{-1} : \quad (2.14)$$

## 2.3 SEMI-ANALYTICAL APPROACH

We can obtain a comprehensive and rather accurate approach of the dynamics of decaying-particle-dominated cosmology, following the arguments of Ref. [17]. At the epoch before the completion of reheating,  $T \approx T_{\text{RH}}$ , the universe is dominated by the number density of which initially has a large value  $n_I$ . Its evolution is given by the exact solution of Eq. (2.1) [24, 25, 29], which at early times, can be written as :

$$n = n_I \frac{R}{R_I}^3 : \quad (2.15)$$

Inserting this into Eq. (2.4), we obtain:

$$H^2 = H_I^2 \frac{R}{R_I}^3; \quad \text{with} \quad H_I^2 = \frac{8}{3M_{\text{P}}^2} m n_I : \quad (2.16)$$

At early times the last term of the left part side of Eq. (2.11) can be safely ignored and it can be easily solved, after substituting Eqs (2.15) and (2.16) in it, with result:

$$f_R = \frac{2}{5} f_{\text{Rc}} R_I^{3/2} R^{5/2} R_I^{5/2}; \quad \text{with} \quad f_{\text{Rc}} = H_I^2 m n_I : \quad (2.17)$$

Combining Eqs (2.17) and (2.6a), we end up with the following relation:

$$T = \frac{12}{2g} f_{\text{Rc}}^{1/4} \frac{R}{R_I}^{3/2} \frac{R}{R_I}^{1/4} : \quad (2.18)$$

The function  $T(R=R_I)$  reaches at (see Fig. 1)

$$\frac{R}{R_{I0}} = 1.48; \quad \text{a maximum value } T_{\text{max}} = 0.767 \frac{12}{2g} f_{\text{RC}}^{1=4} \quad (2.19)$$

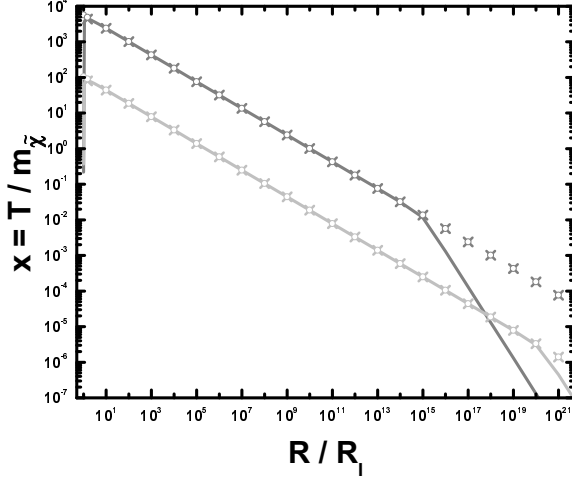


FIGURE 1: The evolution of  $x = T/m_{\tilde{\chi}}$  versus  $R/R_I$ , derived from the numerical solution of Eqs (2.1)-(2.3) (solid lines), from Eq. (2.18) (crosses) and from Eq. (2.20) (open circles) for the parameters of Fig. 2-(a [b]) (normal [light] grey lines, crosses, circles).

of  $R/R_I$  for the case of two representative examples which will be analyzed in sec. 4.1. The solid lines are obtained by using Eq. (2.6a) and the precise numerical solution of Eqs (2.1)-(2.3), whereas crosses [open circles] are from the approximated Eq. (2.18 [2.20]). Good agreement is observed for  $T_{\text{max}} > T > T_{\text{RH}}$  in both cases.

### 3. COLD DARK MATTER ABUNDANCE

The aim of this section is the calculation of  $\Omega_{\tilde{\chi}} h^2$  based on the semi-analytical expressions obtained in the previous section. We assume that  $\tilde{\chi}$  are always nonrelativistic ( $T_{\text{max}} > m_{\tilde{\chi}}$ ) and never in chemical equilibrium after the completion of reheating. The relevant Boltzmann equation is properly reformulated in sec. 3.1. Then two cases are investigated:  $\tilde{\chi}$  reaches (sec. 3.3) or does not reach (sec. 3.2) chemical equilibrium with plasma. The condition which discriminates the two possibilities is specified in sec. 3.2.

#### 3.1 REFORMULATION OF BOLTZMANN EQUATIONS

Our first step is the reexpression of Eq. (2.3) in terms of the variables  $Y^{[\text{eq}]} = n_{\tilde{\chi}}^{[\text{eq}]} = s^{8=3}$  in order to absorb the dilution term. Armed with Eqs (2.20) and (2.21), we are able now to convert the derivatives wrt  $t$ , to derivatives wrt  $x = T/m_{\tilde{\chi}}$ . In fact, supposing that

For  $T < T_{\text{max}}$  the second term in the second parenthesis in Eq. (2.18) can be eliminated. From the resulting expression, we can derive the following useful relations, which signalize the deviation from the standard radiation-dominated evolution. Namely:

i. Scale factor-temperature relation:

$$g^{2=3} R T^{8=3} = \frac{12}{2} f_{\text{RC}}^{2=3} R_I \quad (2.20)$$

Recall that in the radiation-dominated era is the quantity  $g_s^{1=3} (T) R T$  which remains constant.

ii. Expansion rate-temperature relation:

$$H = \frac{2}{12} f_{\text{RC}}^{1=3} g H_I T^4; \quad (2.21)$$

which is obtained by solving Eq. (2.20) wrt  $R$  and inserting it into Eq. (2.16). Note that during the radiation-dominated phase,  $H$  is proportional to  $T^2$  and not to  $T^4$ .

In Fig. 1, we show  $x = T/m_{\tilde{\chi}}$  as a function

$g_s(T)$  and  $g(T)$  vary very little from their values at  $T_{RH}$  and differentiating the constant quantity  $R s^{8=9}$  (see Eq. (2.20) and (2.6b)) wrt  $t$ , we obtain:

$$8\dot{s} = 9Hs; \quad (3.1)$$

Hence, Eq. (2.3) can be rewritten in terms of the new variables as:

$$\dot{Y} = h_{\nu i} Y^2 - Y^{eq2} s^{8=3} + N_{\nu n} s^{11=3}; \quad (3.2)$$

Replacing  $R$  by  $x$  in Eq. (2.15), through Eq. (2.20), we obtain

$$n(x) = n_I(x=x_I)^8; \quad (3.3)$$

with  $x_I = T_I/m_{\nu}$  and  $T_I$  the temperature corresponding to  $R_I$  derived from Eq. (2.20).

Using as independent the variable  $x$  instead of  $t$  in Eq. (3.1), we obtain:

$$Y^0 = \frac{8}{9sH} \frac{ds}{dT} m_{\nu} Y; \quad (3.4)$$

where prim e means derivative wrt  $x$ . Substituting Eqs (2.6b), (2.21) and (3.2) in Eq. (3.4), this reads:

$$Y^0 = Y_n Y^2 - Y^{eq2} x^3 - Y_N x^5; \quad (3.5)$$

$$\text{where } Y_n(x) = \frac{64}{45} \frac{2^2}{45} s^{5=3} H_I^{-1} f_{RC} m_{\nu}^4 g_{01} h_{\nu i} \quad (3.6)$$

$$\text{and } Y_N(x) = \frac{64}{45} \frac{2^2}{45} s^{11=3} H_I^{-1} N_{\nu} f_{RC} n_I x_I^8 m_{\nu}^{-12} g_{01}^0; \quad (3.7)$$

The parameters  $g_{01}$  and  $g_{01}^0$  are defined as follows:

$$g_{01}^0 = g^{1=2} g_s^{5[11]=3} g^{1=2}; \quad \text{with } [11] g^{1=2} = p \frac{g_s}{g} \left( 1 + \frac{T}{3g_s} \frac{dg_s}{dT} \right) \quad (3.8)$$

### 3.2 NON EQUILIBRIUM PRODUCTION

In this case,  $Y = Y^{eq}$  and so,  $Y^2 = Y^{eq2}$ ,  $Y^{eq2}$ . Inserting this into Eq. (3.5) and integrating from  $x_I$  down to  $x_{RH} = T_{RH}/m_{\nu}$ , we arrive at the yield of  $\nu$ ,  $Y(x_{RH}) = Y_{RH}$ :

$$Y_{RH} = Y_n(x_{RH}) + Y_N(x_{RH}); \quad (3.9)$$

$$\text{with } Y_n(x) = \frac{64}{45} \frac{g^2}{(2)^3} \frac{2^2}{45} s^{11=3} H_I^{-1} f_{RC} J_n(x) m_{\nu}^6 \quad (3.10)$$

$$\text{and } Y_N(x) = \frac{64}{45} \frac{2^2}{45} s^{11=3} H_I^{-1} N_{\nu} J_N(x) f_{RC} m_{\nu}^{-12} n_I x_I^8; \quad (3.11)$$

where we have defined the quantities ( $x_I$  can be approximated by infinity, since  $x_I \ll x_{RH}$ ):

$$J_n(x^0) = \int_{x^0}^{\infty} dx x^{10} e^{-2x} P_2^2(1=x) g_s^{16=3} g_{01} h_{\nu i} \quad \text{and} \quad J_N(x^0) = \int_{x^0}^{\infty} dx x^5 g_{01}^0; \quad (3.12)$$

The maximum  $\nu$  particles production takes place at  $x = T/m_{\nu} (= 0.212$ , for constant  $h_{\nu i}$ ), where the integrand of  $J_n$  reaches its maximum [17]. Therefore, the condition which discriminates the EP from the non-EP of  $\nu$  is the following:

$$Y_n(x) + Y_N(x) - Y^{eq}(x) < 0; \quad \text{non-EP} \\ 0; \quad \text{EP} \quad (3.13)$$

## 3.3 EQUILIBRIUM PRODUCTION

In this case, we introduce the notion of freeze out temperature,  $T_F = x_F m \sim [25, 30]$ , which assists us to study Eq. (3.5) in the two extreme regimes:

At very early times, when  $x \ll x_F$ ,  $\tilde{\nu}$ 's are very close to equilibrium. So, it is more convenient to rewrite Eq. (3.5) in terms of the variable  $Y(x) = Y^{\text{eq}}(x)$  as follows:

$$Y^0(x) = Y^{\text{eq}0} + Y_N Y^2 - Y^{\text{eq}2} x^3 - Y_N x^5; \quad (3.14)$$

The freeze-out temperature can be defined by

$$(x_F) = Y^{\text{eq}}(x_F) - Y^2(x_F) - Y^{\text{eq}2}(x_F) = (F + 2) Y^{\text{eq}2}(x_F); \quad (3.15)$$

where  $F$  is a constant of order one determined by comparing the exact numerical solution of Eq. (3.5) with the approximate under consideration. Inserting Eqs (3.15) into Eq. (3.14) and neglecting  $Y^0$  (since,  $Y^0 \approx Y^{\text{eq}0}$ ), we obtain the following equation which can be solved iteratively:

$$\ln Y^{\text{eq}}(x_F) = Y_N F (F + 2) Y^{\text{eq}}(x_F) x_F^3 - Y_N x_F^5 = Y^{\text{eq}}(x_F); \quad (3.16)$$

$$\text{with } Y_N = Y_N(x_F) \text{ and } \ln Y^{\text{eq}}(x) = \frac{1}{x^2} - \frac{13}{2x} - \frac{8g_s^0(x)}{3g_s(x)} \quad (3.17)$$

At late times, when  $x \gg x_F$ ,  $Y \approx Y^{\text{eq}}$  and so,  $Y^2 \approx Y^{\text{eq}2}$ ,  $Y^2 \approx Y^2$ . Inserting this into Eq. (3.5), the yield of  $\tilde{\nu}$  at  $T_{RH}$ ,  $Y_{RH} = Y(x_{RH})$  can be found by solving the resulting differential equation. We distinguish the cases:

i. For  $N_{\tilde{\nu}} = 0$ , the integration from  $x_F$  down to  $x_{RH}$  can be made trivially, with result:

$$Y_{RH} = \frac{1}{Y_F} + \frac{8}{15} \frac{2}{45} M_P^2 m_{\tilde{\nu}}^4 J_F; \quad (3.18)$$

where we have defined the quantities:

$$J_F = \int_{x_{RH}}^{x_F} dx x^3 g_{\text{eff}}^{-1} \text{ and } Y_F = (F + 1) Y^{\text{eq}}(x_F); \quad (3.19)$$

$$\text{with } Y^{\text{eq}}(x) = \frac{g}{(2)^{3=2}} \frac{2}{45} g_s^{8=3} m_{\tilde{\nu}}^5 x^{13=2} e^{-1=x} P_2(1=x); \quad (3.20)$$

The choice  $F = 1.0 \pm 0.2$  provides the best agreement with the precise numerical solution of Eq. (3.5), without to cause dramatic instabilities.

ii. For  $N_{\tilde{\nu}} \neq 0$ , the integration of the resulting equation can be realized numerically. However, using  $g$ 's and  $g$ 's at their values at  $x_{RH}$ , an analytic formula can be derived for this case, also (note that  $x_{RH} < x_F$ ):

$$Y_{RH} = \frac{1}{Y_N(x_{RH}) x_{RH}^4} \left[ 2 + Y_{RH} \tan^{-1} \frac{2 + Y_N(x_{RH}) x_F Y_F}{Y_{RH}} + Y_{RH} \ln \frac{x_{RH}}{x_F} \right]; \quad (3.21)$$

where  $Y_F$  is given by Eq. (3.20) and the quantity  $Y_{RH} = \frac{p}{4 Y(x_{RH}) Y_N(x_{RH})}$  has been defined.

## 3.4 THE CURRENT ABUNDANCE

Our main aim is the calculation of the current  $\tilde{n}$  relic density, which is based on the well known formula [30, 11]:

$$\tilde{n} = \tilde{n}_c^0 = \frac{\tilde{n}}{c} = m_{\tilde{\nu}} s_0 Y_0 = \frac{\tilde{n}}{c}; \quad \text{where } Y_0 = \tilde{n}_c^0 = s_0; \quad (3.22)$$

$\tilde{n}_c^0 = m_{\tilde{\nu}} \tilde{n}_c^0$  is the current  $\tilde{n}$  energy density and  $\tilde{n}_c^0$  and  $s_0$  are the critical energy and entropy density today. With a background radiation temperature of  $T_0 = 2.726 \text{ } ^\circ\text{K}$ , we arrived at the final result:

$$\tilde{n} h^2 = 2.755 \cdot 10^8 \frac{m_{\tilde{\nu}}}{\text{GeV}} Y_0; \quad (3.23)$$

For the numerical program,  $Y_0$  is determined at a value  $R_f$  large enough so as,  $Y_0$  is stabilized to a constant value. For the semi-analytical calculation, we assume that there is no entropy production for  $T < T_{RH}$ . Then, it is convenient to single out the cases:

- i. For  $N_{\tilde{\nu}} = 0$ , there is no  $\tilde{n}$  production for  $x < x_{RH}$ . Therefore, the present yield can be estimated reliably at  $x_{RH}$  with  $Y_0 = Y_{RH} s^{5=3}(x_{RH})$  (in accordance with Ref. [17]).
- ii. For  $N_{\tilde{\nu}} \neq 0$ , the residual (for  $x < x_{RH}$ ) produced  $\tilde{n}$  can annihilate satisfying an equation analog to Eq. (2.3) but in a radiation-dominated background, any more (similarly to the case of Ref. [22]):

$$\tilde{n} + 3H_{RD} \tilde{n} + h_{\nu i} \tilde{n}^2 = \tilde{n}^{eq2} \quad N_{\tilde{\nu}} \tilde{n} = 0; \quad \text{with } H_{RD} = \frac{8}{3M_P^2} \frac{1=2}{R}; \quad (3.24)$$

The equilibrium distribution  $\tilde{n}^{eq}$  can be safely neglected since, as it turns out, is in any case numerically irrelevant. Using the variable  $Y_{RD} = \tilde{n} s$  and the entropy conservation law in the radiation-dominated era, Eq. (3.24) can be rewritten as:

$$Y_{RD}^0 = \frac{ds=dT}{3H_{RD}} m_{\tilde{\nu}} Y_{RD}^2 h_{\nu i} \quad N_{\tilde{\nu}} \tilde{n} s^2; \quad \text{with [11]} \quad \frac{ds=dT}{3H_{RD}} = \frac{r}{45} M_P g^{1=2}; \quad (3.25)$$

The post-late times, i.e. for  $x < x_{RH}$ , evolution of  $\tilde{n}$  can be approximated, using the exact solution of Eq. (2.1) [24], the entropy conservation law and the time-temperature relation [29] in a radiation-dominated era, as follows (the ratio  $x_{RH} = x_I$  can be safely ignored):

$$\tilde{n}(x) = n_{RH} (x=x_{RH})^3 e^{x_{RH}^2 = x^2}; \quad (3.26)$$

where  $n_{RH} = \tilde{n}(x_{RH})$  is given by Eq. (2.15). Inserting Eqs (3.26) and (2.6b) into Eq. (3.25), this can be cast in the following final form:

$$Y_{RD}^0 = Y_{RDn} Y_{RD}^2 \quad Y_{RDn} e^{x_{RH}^2 = x^2} x^3; \quad (3.27)$$

$$\text{where } Y_{RDn}(x) = \frac{r}{45} M_P m_{\tilde{\nu}} g^{1=2} h_{\nu i} \quad (3.28)$$

$$\text{and } Y_{RDn}(x) = \frac{r}{45} \frac{2^2}{45} M_P N_{\tilde{\nu}} n_{RH} x_{RH}^3 m_{\tilde{\nu}}^5 g^{1=2} g_s^2; \quad (3.29)$$

$Y_0$  can be obtained, by solving numerically Eq. (3.27) from  $x_{RH}$  down to 0, with initial condition  $Y_{RD}(x_{RH}) = Y(x_{RH}) s^{5=3}(x_{RH})$ ,  $Y(x_{RH})$  being derived from Eq. (3.21) or (3.9).

Even in the exceptional case, (see sec. 4.2) where  $\tilde{\nu}$  decouples a little after the completion of reheating (i.e. for  $x < x_{RH}$ ), Eq. (3.27) can be applied with  $Y_{RD}(x_{RH}) = 0$ , giving reliable results.

When the first [second] term in the right hand side of Eq. (3.27) evaluated at  $x_{RH}$  dominates over the second [first] one, an analytical solution of Eq. (3.27) can be easily derived, which works frequently well, as we will see in sec. 4.2:

$$\text{a) } Y_0 = \frac{Y_{RD}(x_{RH})}{1 + Y_{RDn}(x_{RH})Y_{RD}(x_{RH})x_{RH}} \quad \text{b) } Y_0 = Y_{RD}(x_{RH}) + \frac{Y_{RDn}(x_{RH})^{\frac{1}{h}}}{2ex_{RH}} \quad (3.30)$$

where, as in the case of Eq. (3.21),  $h$ ,  $\nu_i$  and  $g$ 's have been fixed at their values at  $x_{RH}$ .

Practically, since an unavoidable discrepancy enters between the input  $x_{RH}$  and the output  $x_{rh} = T_{rh} = m_{\tilde{\nu}}$  (i.e., the solution of Eq. (2.7)),  $x_{RH}$  in Eqs (3.26) (3.27) and (3.29) is to be replaced by a matching scale  $x = x_{RH} = T_{RH}$  with  $T_{RH} = 1.25 - 0.65$ , in order for the solution of Eq. (3.27) to match better the solution of the system of Eqs (2.1)-(2.3). Although we did not succeed to achieve a general analytical solution of Eq. (3.27), we consider as a significant development the derivation of a result for our problem by solving numerically just one equation, instead of the whole system above.

#### 4. APPLICATIONS

Our numerical investigation depends on the parameters:

$$m_{\tilde{\nu}}; N_{\tilde{\nu}}; T_{RH}; m_{\tilde{\nu}}; h \nu_i :$$

Note that the numerical choice of  $n_I$  turns out to be irrelevant for the result of  $\tilde{\nu}h^2$ . Just for definiteness we determine it, through  $m_{\tilde{\nu}}$  using Eq. (2.16) with  $H_I = m_{\tilde{\nu}}$  as in the simplest model of chaotic inflation [20, 19]. Alternatively  $T_{RH}$  and  $m_{\tilde{\nu}}$  can be related through a coefficient which includes an effective suppression scale of the interaction of  $\tilde{\nu}$ ,  $M_e$  and the coupling of  $\tilde{\nu}$  and  $\tilde{\nu}$ , [21, 26]. However, since we examine the problem from cosmological point of view, we prefer to handle  $m_{\tilde{\nu}}$  and  $T_{RH}$  as input parameters without any further reference to  $M_e$  and  $\tilde{\nu}$ , which are obviously Particle Physics model dependent. In our scanning we take into account the following bounds:

$$\text{a) } m_{\tilde{\nu}} = 10^3 \text{ GeV}; \quad \text{b) } N_{\tilde{\nu}} = 1 \quad \text{and} \quad \text{c) } T_{RH} = 0.001 \text{ GeV} : \quad (4.1)$$

The bound of Eq. (4.1a) is just conventional, this of Eq. (4.1b) comes from the arguments of the appendix of Ref. [21] and this of Eq. (4.1c) from the requirement not to spoil the successful predictions of Big Bang nucleosynthesis.

Model dependent is also the derivation of  $h \nu_i$  from  $m_{\tilde{\nu}}$  and the residual SUSY spectrum. To keep our presentation as general as possible, we decide to treat  $m_{\tilde{\nu}}$  and  $h \nu_i$  as unrelated input parameters, choosing plausible (from SUSY models point of view) values for them. Namely, we focus our attention on the ranges:

$$\text{a) } 200 \text{ GeV} < m_{\tilde{\nu}} < 500 \text{ GeV} \quad \text{and} \quad \text{b) } 10^{12} \text{ GeV}^2 < h \nu_i < 10^8 \text{ GeV}^2 : \quad (4.2)$$

The lower bound in Eq. (4.2a) arises roughly from the LEP bound on Higgs mass (see, e.g. Ref. [2]), whereas the upper is imposed in order the analyzed range to be possibly

detectable in the future experiments (see, e.g. Ref. [31]). On the other hand,  $h \nu_i$  of the range of Eq. (4.2b) can be naturally produced in the context of SUSY models. The lower value can be derived in the case of a bino LSP or slepton coannihilations whereas the upper, in the case of a wino LSP or coannihilations with squarks or gauginos or of A-pole effect. Note that possible specification of the p-wave suppression in the case of a bino LSP do not alter essentially our results.

In sec. 4.1 we will illustrate the two kinds of  $\tilde{\nu}$  production and in sec. 4.2 we will compare the results of our numerical and semi-analytical  $\tilde{\nu}h^2$  calculations. Finally, in sec. 4.3 we will present areas compatible with Eq. (1.2).

#### 4.1 EQUILIBRIUM VERSUS NON-EQUILIBRIUM PRODUCTION

FIGURE	2-(a <sub>1</sub> ;a <sub>2</sub> )	2-(b <sub>1</sub> ;b <sub>2</sub> )
INPUT PARAMETERS		
$m_{[\tilde{\nu}]} = 10^6 [350] \text{ GeV}; h \nu_i = 10^{10} \text{ GeV}^2$		
$x_{RH}$	5/350	0.001/350
$N_{\tilde{\nu}}$	$1.2 \cdot 10^8$	$1.05 \cdot 10^2$
$g(x_{RH})$	10.88	3.36
$g_s(x_{RH})$	10.85	3.91
OUTPUT PARAMETERS		
$\tilde{\nu}$ -DECOUPLING		
$(Y_n + Y_N)(x)$	$1.4 \cdot 10^{10}$	$2.0 \cdot 10^{18}$
$Y^{eq}(x)$	$2.8 \cdot 10^{16}$	$2.8 \cdot 10^{16}$
PRECISE REHEATING		
$x_{max}$	4378.2	80.4
$x_{th}$	4.52/350	0.0009/350
$(x_{th}) (\text{GeV}^4)$	11826.3	$2.3 \cdot 10^{12}$
$(R=R_I)_{th}$	$8.06 \cdot 10^4$	$1.38 \cdot 10^{20}$

TABLE 1: Input and output parameters for the two examples illustrated in Figs. 1 and 2-(a, b)

of  $\tilde{\nu}h^2$  in Eq. (1.1). The distinguish is realized by explicitly applying the criterion of Eq. (3.13) for  $x = 74.2=350$  (see Table 1) and is illustrated in Figs 2-(a<sub>1</sub>;b<sub>1</sub>). Higher  $T_{RH}$ , and consequently, (see sec. 4.2) lower  $N_{\tilde{\nu}}$  are required for EP. In this case, the freeze out condition in Eq. (3.16) gives  $x_F = 17.22=350 > x_{RH}$ . The choice  $x_{RH} = 0.89 [0.72]$  allows us to reach the numerical solution of Eq. (2.1)–(2.3), by solving Eq. (3.27) or employing the approximated Eq. (3.30a [b]) for [non]EP.

As is shown in Fig. 1 and in Table 1,  $x_{max} = T_{max} = m_{\tilde{\nu}}$  is much greater than  $x_{th}$ , which is derived by solving Eq. (2.7) and corresponds to  $(R=R_I)_{th} = (R=R_I)_0$  resulting to  $(x_{th}) = R(x_{th})$  (see Figs 2-(a<sub>2</sub>;b<sub>2</sub>)). We observe that  $x_{th}$  is quite close to  $x_{RH}$ , mainly due to our definition in Eq. (2.8). On the contrary, if we had adopted (as in Ref. [17]), the instantaneous conversion of  $\tilde{\nu}$  to  $R$ , the later discrepancy would have been much more sizeable, causing an equally significant instability on the  $\tilde{\nu}h^2$  calculation, too.

The operation of the two fundamental phenomena described in our work (i.e., the  $\tilde{\nu}$  [non]EP and the reheating) are instructively displayed in Figs. 2-(a [b]). Namely, in Figs 2-(a<sub>1</sub>;b<sub>1</sub>), we depict the neutralino yield  $Y_{\tilde{\nu}=S}^{[eq]}$  (solid [dotted] lines) and in Figs 2-(a<sub>2</sub>;b<sub>2</sub>), the [radiation] energy density  $\rho_{[R]}$  (dashed [dot-dashed] lines) versus  $x$  (we prefer  $Y_{\tilde{\nu}=S}^{[eq]}$  instead of  $Y_{(RD)}^{[eq]}$ , since it offers a unified prescription of the evolution before and after  $x_{RH}$ ). The needed for our calculation inputs and some key-outputs are comparatively listed in the Table 1.

In both cases, we used the same  $m_{\tilde{\nu}}$  and we fixed  $m_{\tilde{\nu}}$  and  $h \nu_i$  in the middle of the ranges of Eq. (4.2). By adjusting  $T_{RH}$  and  $N_{\tilde{\nu}}$ , we achieve EP or non-EP, extracting the central value

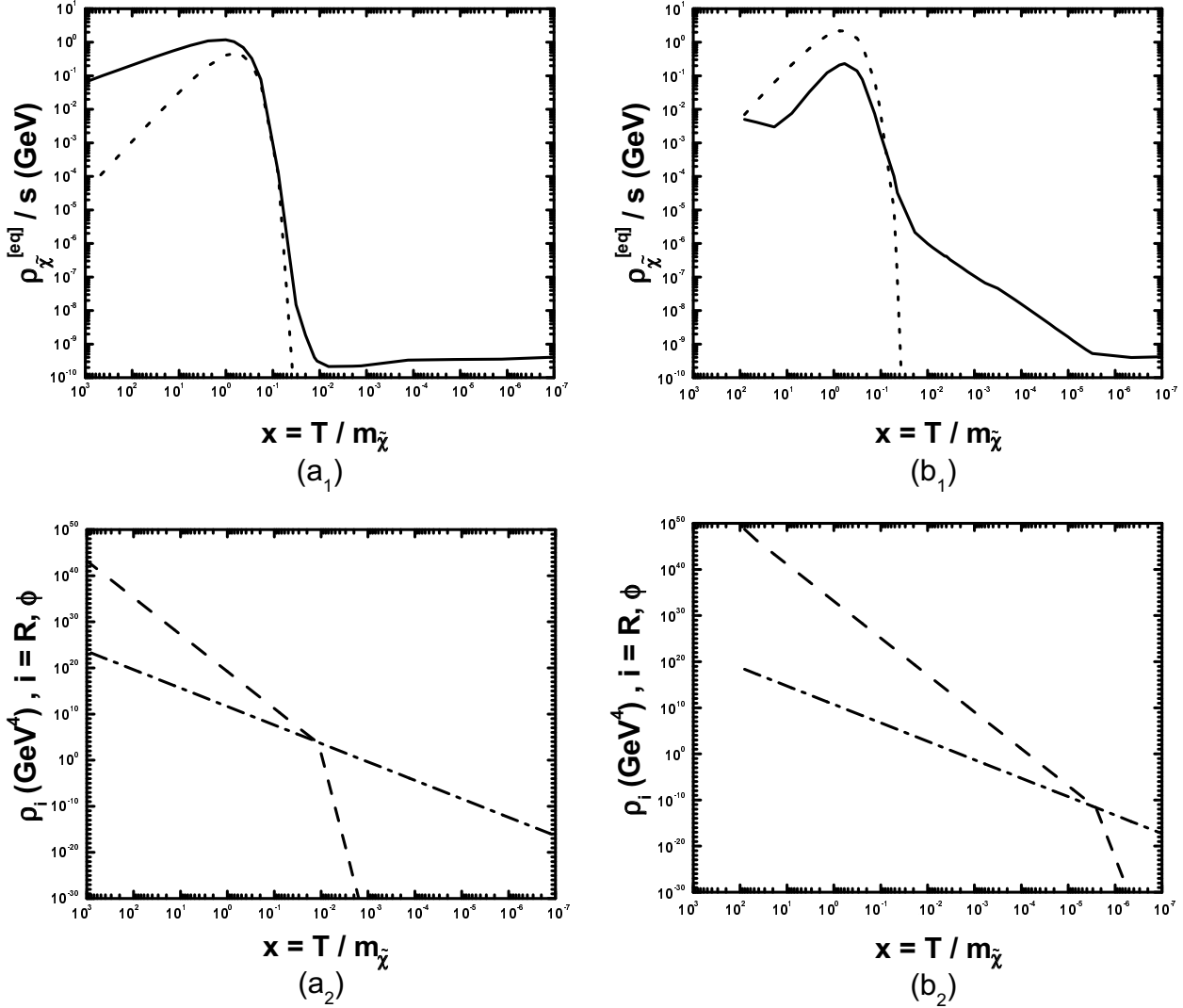


FIGURE 2: (a<sub>1</sub>;b<sub>1</sub>) The neutralino yield  $\rho_{\tilde{\chi}}^{[eq]}=s$  (solid [dotted] line) and (a<sub>2</sub>;b<sub>2</sub>) the [radiation] energy densities  $\rho_{[R,\phi]}$  (dashed [dot dashed] line) versus  $x = T/m_{\tilde{\chi}}$ . We take  $m_{\tilde{\chi}} = 10^6$  GeV;  $m_{\tilde{g}} = 350$  GeV;  $h_{\nu i} = 10^{10}$  GeV<sup>2</sup> and  $T_{RH} = 5$  GeV;  $N_{\tilde{\chi}} = 1.2 \cdot 10^8$  (a<sub>1</sub>;a<sub>2</sub>) for equilibrium production or  $T_{RH} = 0.001$  GeV;  $N_{\tilde{\chi}} = 1.05 \cdot 10^3$  (b<sub>1</sub>;b<sub>2</sub>) for non-equilibrium production. In both cases, we extract  $\Omega_{\tilde{\chi}} h^2 = 0.11$ .

#### 4.2 NUMERICAL VERSUS SEMI-ANALYTICAL RESULTS

The validity of our semi-analytical approach can be tested by comparing its results for  $\Omega_{\tilde{\chi}} h^2$  with those obtained by the numerical solution of Eq. (2.1)–(2.3). In addition, useful conclusions can be deduced for the behavior of  $\Omega_{\tilde{\chi}} h^2$  as a function of our free parameters and the regions where each  $\tilde{\chi}$ -production mechanism can be activated.

Our results are presented in Fig. 3. The solid lines are from our numerical code, whereas crosses are obtained by employing (with  $\Gamma_F = 1$ ) Eq. (3.9 [3.21]) for [non]EP and solving numerically Eq. (3.27) with a convenient  $T_{RH}$  (comments on the validity of Eq. (3.30) are given, too). The type of  $\tilde{\chi}$ -production and the chosen  $T_{RH}$ 's for the parameters used in Fig. 3 are arranged in Table 2.

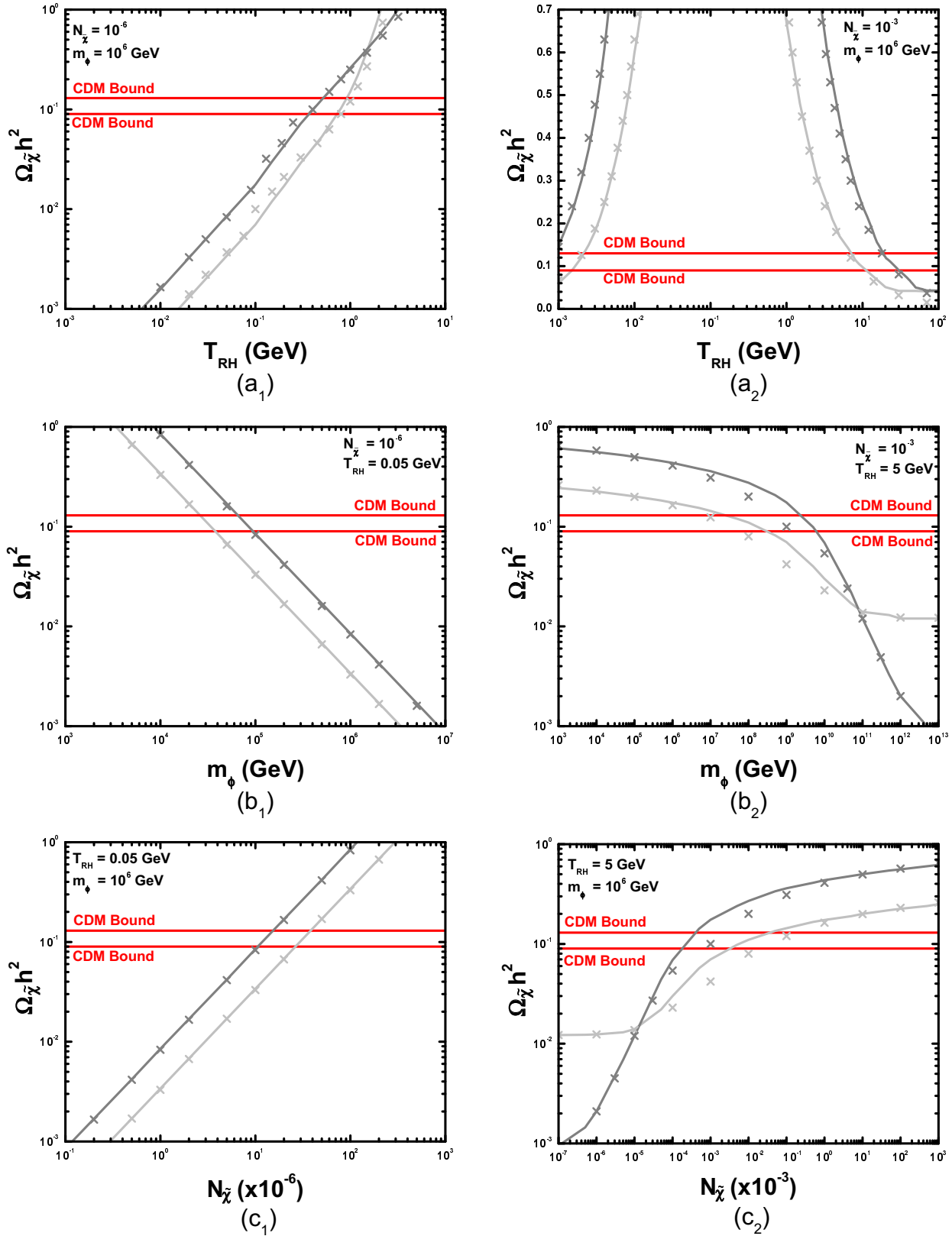


FIGURE 3:  $\Omega_{\tilde{\chi}} h^2$  versus  $T_{RH}$  (a<sub>1</sub>;a<sub>2</sub>),  $m_{\phi}$  (b<sub>1</sub>;b<sub>2</sub>) and  $N_{\tilde{\chi}}$  (c<sub>1</sub>;c<sub>2</sub>) for fixed (indicated in the graphs)  $N_{\tilde{\chi}}$  and  $m_{\phi}$ ,  $N_{\tilde{\chi}}$  and  $T_{RH}$ ,  $T_{RH}$  and  $m_{\phi}$  correspondingly. We take  $m_{\tilde{\chi}} = 200$  [500] GeV (light [normal] grey lines and crosses) and  $h_{\nu i} = 10^{12}$  [ $10^8$ ] GeV<sup>2</sup> (a<sub>1</sub>;b<sub>1</sub>;c<sub>1</sub> [a<sub>2</sub>;b<sub>2</sub>;c<sub>2</sub>]). The solid lines [crosses] are obtained by our numerical code [semi-analytical expressions].

FIG .	RANGES OF X-AXIS PARAMETERS		~PRO- DUCTION	R <sub>H</sub>
	m <sub>~</sub> = 200 GeV	m <sub>~</sub> = 500 GeV		
3-(a <sub>1</sub> )	(0.001 0.08) GeV (0.08 2) GeV	(0.001 0.12) GeV (0.12 3) GeV	non-EP EP	0.7 1.0
3-(b <sub>1</sub> )	(10 <sup>3</sup> 10 <sup>7</sup> ) GeV		non-EP	0.7
3-(c <sub>1</sub> )	10 <sup>7</sup> 10 <sup>3</sup>		non-EP	0.7
3-(a <sub>2</sub> )	(0.001 0.05) GeV (2 50) GeV	(0.002 0.01) GeV (2 50) GeV	EP EP	1.3 1.9
3-(b <sub>2</sub> )	(10 <sup>3</sup> 10 <sup>8</sup> ) GeV (10 <sup>9</sup> 10 <sup>13</sup> ) GeV		EP EP	1.9 0.9
3-(c <sub>2</sub> )	10 <sup>10</sup> 10 <sup>6</sup> 10 <sup>6</sup> 1		EP EP	0.9 1.9

TABLE 2: The type of  $\tilde{\nu}$ -production and the chosen  $R_H$ 's for various ranges of the x-axis parameters and  $m_{\tilde{\nu}}$ 's in Fig. 3 (the use of 0.7 is extended a little beyond the indicated regions).

The light [normal] grey lines and crosses correspond to  $m_{\tilde{\nu}} = 200$  [500] GeV. In Fig. 3-(a<sub>1</sub>;b<sub>1</sub>;c<sub>1</sub> [a<sub>2</sub>;b<sub>2</sub>;c<sub>2</sub>]), we fixed  $h_{\nu i} = 10^{12}$  [ $10^8$ ] GeV<sup>2</sup>. We design  $\tilde{\nu}h^2$  versus:

$T_{RH}$ , in Fig. 3-(a<sub>1</sub> [a<sub>2</sub>]) for  $N_{\tilde{\nu}} = 10^6$  [ $10^3$ ] and  $m_{\tilde{\nu}} = 10^6$  GeV. Comparing these  $\tilde{\nu}h^2$  and taking into account the information of Table 2, we deduce that non-EP is accommodated for lower  $h_{\nu i}$  and  $T_{RH}$  and higher  $m_{\tilde{\nu}}$ , since in these cases,  $Y_n$  [ $Y_N$ ] in Eq. (3.10 [3.11]) decrease, facilitating the satisfaction of Eq. (3.13) for non-EP.  $N_{\tilde{\nu}}$  allows us to produce acceptable results for  $\tilde{\nu}h^2$  even for non-EP, in contrast with the findings of Ref. [18], where  $N_{\tilde{\nu}}$  was fixed to 0, by assumption. When  $\tilde{\nu}h^2$  is increasing function of  $T_{RH}$ , Eq. (3.30b) works well. However, for larger  $h_{\nu i}$  and/or  $T_{RH}$ ,  $\tilde{\nu}h^2$  decreases when  $T_{RH}$  increases (Fig. 3-(a<sub>2</sub>)). None of the expressions in Eq. (3.30) works in this regime and so, the numerical solution of Eq. (3.27) is indispensable. For  $m_{\tilde{\nu}} = 200$  [500] GeV;  $h_{\nu i} = 10^8$  GeV<sup>2</sup> and  $T_{RH} > 8.8$  [22.5] GeV,  $\tilde{\nu}$  decouples for  $x < x_{RH}$ .

$m_{\tilde{\nu}}$ , in Fig. 3-(b<sub>1</sub> [b<sub>2</sub>]) for  $N_{\tilde{\nu}} = 10^6$  [ $10^3$ ] and  $T_{RH} = 0.05$  [5] GeV. In both cases,  $\tilde{\nu}h^2$  decreases as  $m_{\tilde{\nu}}$  increases. Eq. (3.27b [a]) gives reliable results for  $m_{\tilde{\nu}} > 10^9$  and  $m_{\tilde{\nu}} = 500$  [200] GeV in Fig. 3-(b<sub>2</sub>) and for the parameters of Fig. 3-(b<sub>1</sub>).

$N_{\tilde{\nu}}$ , in Fig. 3-(c<sub>1</sub> [c<sub>2</sub>]) for  $T_{RH} = 0.05$  [5] GeV and  $m_{\tilde{\nu}} = 10^6$  GeV. We observe that  $\tilde{\nu}h^2$  increases with  $N_{\tilde{\nu}}$ . Eq. (3.27b [a]) gives reliable results for  $N_{\tilde{\nu}} < 10^6$  and  $m_{\tilde{\nu}} = 500$  [200] GeV in Fig. 3-(c<sub>2</sub>) and for the parameters of Fig. 3-(c<sub>1</sub>).

Comparing Fig. 3-(b<sub>1</sub> [b<sub>2</sub>]) and Fig. 3-(c<sub>1</sub> [c<sub>2</sub>]), it can be induced that  $\tilde{\nu}h^2$  remains invariant for constant  $N_{\tilde{\nu}}m_{\tilde{\nu}}^{-1}$ . This can be understood by the observation that  $y_N$  in Eq. (3.7) is proportional to this quantity. The adjustment of  $R_H$  turns out to be crucial, in order for the results from the semi-analytical treatment to approach the numerical ones. However, this kind of uncertainties is unavoidable to such approximations (see Ref. [17]). Note that the accuracy of our approximations increases as  $N_{\tilde{\nu}}m_{\tilde{\nu}}^{-1}$  is reduced.

#### 4.3 ALLOWED REGIONS

Requiring  $\tilde{\nu}h^2$  to be confined in the cosmologically allowed range of Eq. (1.2), one can restrict the free parameters. The data is derived exclusively by the numerical program.



Our results are presented in Fig. 4. The light (normal) grey regions are constructed for  $m_{\tilde{\nu}} = 200$  [500] GeV. In Fig. 4-(a<sub>1</sub>; b<sub>1</sub>; c<sub>1</sub>) [a<sub>2</sub>; b<sub>2</sub>; c<sub>2</sub>], we fixed  $h_{\nu} = 10^{12}$  [ $10^8$ ] GeV<sup>2</sup>. We display the allowed region on the:

$N_{\tilde{\nu}} - T_{RH}$  plane, in Fig. 4-(a<sub>1</sub>; a<sub>2</sub>) for  $m_{\tilde{\nu}} = 10^6$  GeV. Since  $\Omega_{\tilde{\nu}} h^2$  increases with  $T_{RH}$  for low  $h_{\nu}$ 's, the increase of  $T_{RH}$  requires diminution of  $N_{\tilde{\nu}}$  in Fig. 4-(a<sub>1</sub>). On the contrary, in Fig. 4-(a<sub>2</sub>), when decrease of  $\Omega_{\tilde{\nu}} h^2$  is achieved with increase of  $T_{RH}$  for  $T_{RH} \gtrsim 2$  GeV, augmentation of  $N_{\tilde{\nu}}$  is needed for increasing  $T_{RH}$ .

$N_{\tilde{\nu}} - m_{\tilde{\nu}}$  plane, in Fig. 4-(b<sub>1</sub>; b<sub>2</sub>) for  $T_{RH} = 0.05$  [5] GeV. Since in both cases,  $\Omega_{\tilde{\nu}} h^2$  [de]creases as  $N_{\tilde{\nu}}$  [m] increases, increase of  $N_{\tilde{\nu}}$  requires increase of  $m_{\tilde{\nu}}$ .

$T_{RH} - m_{\tilde{\nu}}$  plane, in Fig. 4-(c<sub>1</sub>; c<sub>2</sub>) for  $N_{\tilde{\nu}} = 10^6$  [ $10^3$ ]. Since for  $T_{RH} \lesssim 2$  GeV, increase of  $T_{RH}$  causes increase of  $\Omega_{\tilde{\nu}} h^2$  (see Fig. 3-(a<sub>1</sub>; a<sub>2</sub>))  $m_{\tilde{\nu}}$  is to increase with  $T_{RH}$ , in this regime as in Fig. 4-(c<sub>1</sub>). Similar region exists, also, for the parameters used in Fig. 4-(c<sub>2</sub>). However, for the sake of illustration, in Fig. 4-(c<sub>2</sub>), we concentrated on the regions with  $T_{RH} \gtrsim 2$  GeV. In these, increase of  $m_{\tilde{\nu}}$  is required with decrease of  $T_{RH}$ , since it causes increase of  $\Omega_{\tilde{\nu}} h^2$ , as shown in Fig. 3-(a<sub>2</sub>). The upper [lower] bounds of the allowed areas are derived from the saturation of Eq. (1.2a [b]) (inversely to all other cases).

## 5. CONCLUSIONS-OPEN ISSUES

We considered a deviation from the standard cosmological situation according to which the CDM candidate,  $\tilde{\nu}$  decouples from the plasma (i) during the radiation-dominated era (i.e. after reheating) (ii) being in equilibrium (iii) produced through thermal scatterings. On the contrary, we assumed that  $\tilde{\nu}$  decoupling occurs (i<sup>0</sup>) during a decaying massive particle dominated era (and mainly before reheating) (ii<sup>0</sup>) being or not in equilibrium with the thermal bath (iii<sup>0</sup>) produced by thermal scatterings and directly from the decay.

We solved the problem (i) numerically, integrating the relevant system of the differential equations (ii) semi-analytically, producing approximate relations for the cosmological evolution before reheating and solving the properly re-formulated Boltzmann equations. The second way certainly facilitates the understanding of the physical problem and gives, in most cases, sufficiently accurate results, provided a suitable  $T_{RH}$  is chosen. The variation of  $\Omega_{\tilde{\nu}} h^2$  with respect our free parameters ( $m_{\tilde{\nu}}$ ;  $N_{\tilde{\nu}}$ ;  $T_{RH}$ ) was investigated and regions consistent with the present CDM bounds are constructed, using  $m_{\tilde{\nu}}$ 's and  $h_{\nu}$ 's commonly allowed in SUSY models.

Our formalism can be easily extended to include coannihilations and pole effects. Therefore, it can become applicable for the calculation of  $\Omega_{\tilde{\nu}} h^2$  in the context of specific SUSY models. Also, these scenarios can assist us to the reduction of  $\Omega_{\tilde{\nu}} h^2$  in cases, where it turns out to be even more enhanced than in the standard scenario, as in the presence of Quintessence [32]. Similar analysis of  $\tilde{\nu}$ -decoupling during the extra dimensional cosmological evolution [33] may be also, possible.

## ACKNOWLEDGMENTS

The author gratefully acknowledges A. Riotto, S. Khalil and A. Masiero for inspiring discussions, G. Lazarides, T. Moroi and N. D. Vlachos for useful correspondence. This work was supported by European Union under the RTN contract HPRN-CT-2000-00152.

## REFERENCES

- [1] C.L. Bennet et al, astro-ph/0302207; D.N. Spergel et al, astro-ph/0302209.
- [2] For a particle physics point of view review, see  
A.B. Lahanas, N.E. Mavromatos and D.V. Nanopoulos, hep-ph/0308251.
- [3] H.G. Goldberg, Phys. Rev. Lett. 50, 1419 (1983); J.R. Ellis, J.S. Hagelin, D.V. Nanopoulos,  
K.A. Olive and M. Srednicki, Nucl. Phys. B 238, 453 (1984).
- [4] G.L. Kane, C. Kolda, L. Roszkowski and J.D. Wells, Phys. Rev. D 49, 6173 (1994)  
[hep-ph/9312272].
- [5] J. Ellis, T. Falk and K.A. Olive, Phys. Lett. B 444, 367 (1998) [hep-ph/9810360].
- [6] M.E. Gomez, G. Lazarides and C. Pallis, Phys. Rev. D 61, 123512 (2000) [hep-ph/9907261];  
Phys. Lett. B 487, 313 (2000) [hep-ph/0004028].
- [7] C. Boehm, A. Djouadi and M. Drees, Phys. Rev. D 62, 035012 (2000) [hep-ph/9911496].
- [8] J. Edsjo, M. Schelke, P. Ullio and P. Gondolo, JCAP 04, 001 (2003) [hep-ph/0301106].
- [9] A.B. Lahanas, D.V. Nanopoulos and V.C. Spanos, Phys. Rev. D 62, 023515 (2000)  
[hep-ph/9909497].
- [10] J. Ellis, T. Falk, K.A. Olive and Y. Santoso, Nucl. Phys. B 652, 259 (2003) [hep-ph/0210205].
- [11] J. Edsjo and P. Gondolo, Phys. Rev. D 56, 1879 (1997) [hep-ph/9704361].
- [12] A. Birkedal-Hansen and B.D. Nelson, Phys. Rev. D 67, 095006 (2003) [hep-ph/0211071].
- [13] C. Pallis, Nucl. Phys. B 678, 398 (2004) [hep-ph/0304047].
- [14] T. Gerghetta, G.F. Giudice and J.D. Wells, Nucl. Phys. B 559, 27 (1999) [hep-ph/9904378].
- [15] U. Chattopadhyay and D.P. Roy, Phys. Rev. D 68, 033010 (2003) [hep-ph/0304108].
- [16] J. McDonald, Phys. Rev. D 43, 1063 (1991).
- [17] G.F. Giudice, E.W. Kolb and A. Riotto, Phys. Rev. D 64, 023508 (2001) [hep-ph/0005123].
- [18] N. Fornengo, A. Riotto and S. Scopel, Phys. Rev. D 67, 023514 (2003) [hep-ph/0208072].
- [19] D.J.H. Chung, E.W. Kolb and A. Riotto, Phys. Rev. D 60, 063504 (1999) [hep-ph/9809453].
- [20] B. de Carlos, J.A. Casas, F. Quevedo and E. Roulet, Phys. Lett. B 318, 447 (1993)  
[hep-ph/9308325].
- [21] T. Moroi and L. Randall, Nucl. Phys. B 570, 455 (2000) [hep-ph/9906527].
- [22] M. Fujii and K. Hamaguchi, Phys. Rev. D 66, 083501 (2002) [hep-ph/0205044];  
M. Fujii and M. Ibe, hep-ph/0308118.
- [23] R. Jeannerot, X. Zhang and R. Brandenberg, JHEP 12, 003 (1999) [hep-ph/9901357].
- [24] R.J. Scherrer and M.S. Turner, Phys. Rev. D 31, 681 (1985).
- [25] E.W. Kolb and M.S. Turner, *The Early Universe*, Redwood City, USA: Addison-Wesley (1990).
- [26] S. Khalil, C. Muñoz and E. Torrente-Lujan, New J. Phys. 4, 27 (2002) [hep-ph/0202139].
- [27] G. Belanger, F. Boudjema, A. Pukhov and A. Semenov, Comput. Phys. Commun. 149, 103  
(2002) [hep-ph/0112278].
- [28] P. Gondolo, J. Edsjo, P. Ullio, L. Bergstrom, M. Schelke and E. Baltz, astro-ph/0211238.
- [29] G. Lazarides, Lect. Notes Phys. 592, 351 (2002) [hep-ph/0111328].
- [30] P. Gondolo and G. Gelmini, Nucl. Phys. B 360, 145 (1991).
- [31] C. Muñoz, hep-ph/0309346.
- [32] P. Salati, Phys. Lett. B 571, 121 (2003) [astro-ph/0207396].
- [33] P. Binetruy, C. D'effayet and D. Langlois, Nucl. Phys. B 565, 269 (2000) [hep-th/9905012].